The Plant Cell, Vol. 18, 397–411, February 2006, www.plantcell.org © 2005 American Society of Plant Biologists

Arabidopsis ACCELERATED CELL DEATH2 Modulates Programmed Cell Death [W]

Nan Yao[1] and Jean T. Greenberg[2]

Department of Molecular Genetics and Cell Biology, University of Chicago, Chicago, Illinois 60637

The *Arabidopsis thaliana* chloroplast protein ACCELERATED CELL DEATH2 (ACD2) modulates the amount of programmed cell death (PCD) triggered by *Pseudomonas syringae* and protoporphyrin IX (PPIX) treatment. In vitro, ACD2 can reduce red chlorophyll catabolite, a chlorophyll derivative. We find that ACD2 shields root protoplasts that lack chlorophyll from light- and PPIX-induced PCD. Thus, chlorophyll catabolism is not obligatory for ACD2 anti-PCD function. Upon *P. syringae* infection, ACD2 levels and localization change in cells undergoing PCD and in their close neighbors. Thus, ACD2 shifts from being largely in chloroplasts to partitioning to chloroplasts, mitochondria, and, to a small extent, cytosol. ACD2 protects cells from PCD that requires the early mitochondrial oxidative burst. Later, the chloroplasts of dying cells generate NO, which only slightly affects cell viability. Finally, the mitochondria in dying cells have dramatically altered movements and cellular distribution. Overproduction of both ACD2 (localized to mitochondria and chloroplasts) and ascorbate peroxidase (localized to chloroplasts) greatly reduces *P. syringae*–induced PCD, suggesting a pro-PCD role for mitochondrial and chloroplast events. During infection, ACD2 may bind to and/or reduce PCD-inducing porphyrin-related molecules in mitochondria and possibly chloroplasts that generate reactive oxygen species, cause altered organelle behavior, and activate a cascade of PCD-inducing events.

INTRODUCTION

Programmed cell death (PCD) is a common response to pathogens in higher eukaryotes. In plants, infection by the bacterial pathogen *Pseudomonas syringae* leads to the activation of PCD that can occur very rapidly when it is associated with disease resistance. This rapid PCD is called the hypersensitive response (HR). It occurs when the plant and the pathogen have cognate *Resistance* and *Avirulence* genes, respectively. In the absence of the HR, *P. syringae* also causes cell death (susceptible cell death), albeit at a slower rate. Although initially thought to be entirely distinct types of cell death, both the HR and susceptible cell death can have apoptotic features (Greenberg and Yao, 2004). Furthermore, at least one signaling protein is important for both types of cell death (del Pozo et al., 2004). When an HR occurs in a viral infection, it reduces viral replication (Hatsugai et al., 2004).

Although activation of rapid cell death during the HR can protect plants from at least some pathogens, excessive PCD compromises plant fitness. Several mechanisms exist to limit PCD in plants during infection and possibly other types of stress. For example, loss of the *LESIONS SIMULATING DISEASE1* (*LSD1*) and *ACCELERATED CELL DEATH1* (*ACD1*) or *ACD2* genes leads to runaway cell death, implicating these genes in cell death control (Greenberg and Ausubel, 1993; Dietrich et al., 1994; Greenberg et al., 1994). These mutants require long-day conditions or light for their cell death phenotypes (Dietrich et al., 1994; Asai et al., 2000; Mach et al., 2001; Yang et al., 2004). LSD1 and the related LSD-ONE-like proteins are important for redox sensing (Epple et al., 2003). LSD1 has been implicated in the acclimation of *Arabidopsis thaliana* to light conditions that promote excess light energy (Mateo et al., 2004). ACD1 and ACD2 may control products of chlorophyll breakdown that induce PCD (Mach et al., 2001; Pruzinska et al., 2003). These products may be liberated during infection. Recently, the process of autophagy was also implicated in suppressing PCD during infection in both the primary infected tissue and the systemic uninfected portions of the plant (Greenberg, 2005; Liu et al., 2005). Autophagy is a conserved process in which cellular material is engulfed in double membrane vesicles and eventually degraded.

The *Arabidopsis ACD2* gene encodes a protein also called red chlorophyll catabolite reductase (RCCR) that in vitro can break down red chlorophyll catabolite (RCC). RCC is thought to be an intermediate in the chlorophyll breakdown pathway (Matile et al., 1999). The ACD2 protein can be imported into chloroplasts in vitro (Wüthrich et al., 2000) and localizes to chloroplasts in mature leaves (Mach et al., 2001). In young seedlings, ACD2 localizes to both chloroplasts and mitochondria and appears to be differentially processed and/or utilizes two different start sites (Mach et al., 2001). Overproduction of ACD2 reduces disease symptoms and cell death caused by virulent *P. syringae* infection

[1] Current address: State Key Laboratory of Biocontrol, College of Life Sciences, Sun Yat-sen University, Guangzhou 510275, People's Republic of China.

[2] To whom correspondence should be addressed. E-mail jgreenbe@uchicago.edu; fax 773-702-9270.

The author responsible for distribution of materials integral to the findings presented in this article in accordance with the policy described in the Instructions for Authors (www.plantcell.org) is: Jean T. Greenberg (jgreenbe@uchicago.edu).

[W] Online version contains Web-only data.

Article, publication date, and citation information can be found at www.plantcell.org/cgi/doi/10.1105/tpc.105.036251.

(Mach et al., 2001). *acd2* mutants show excessive cell death during infection and can show spontaneous spreading cell death (Greenberg et al., 1994). Together, these findings raised the possibility that chlorophyll breakdown products modulate cell death during infection.

We recently characterized PCD in *acd2* mutant, wild-type, and ACD2-overexpressing plants by inducing cell death with various stimuli. We sought to characterize the PCD process that ACD2 affects and understand the mode of action of selected endogenous cell death inducers. Protoplasts lacking ACD2 die in response to light with an apoptotic morphology that includes chromatin condensation and the induction of DNA fragmentation within subregions of their nuclei (Yao et al., 2004). The requirement for light is likely due to the photoactivation of an ACD2 substrate that causes PCD. The possible endogenous substrate of ACD2, RCC, has the chemical properties expected for a molecule that can be photoactivated (Greenberg and Yao, 2004). Light-dependent cell death in *acd2* mutant cells requires protein synthesis (Asai et al., 2000; Mach et al., 2001; Yao et al., 2004). Thus, the photoactivation of ACD2 substrates likely does not directly kill cells but activates a death program requiring new protein synthesis. A similar phenomenon has been described to occur in the *flu* mutant that accumulates protochlorophyllide (Wagner et al., 2004).

To test whether RCC causes PCD, we previously sought to treat *acd2*, wild-type, and ACD2-overproducing plants with synthetic RCC and quantitate PCD. However, because RCC was not available, we characterized the affects of protoporphyrin IX (PPIX) and pheophorbide A, molecules that are formed upstream of RCC in the chlorophyll biosynthetic and catabolic pathways, respectively. PPIX is known to be photoactivated to cause PCD in animals through the production of singlet oxygen. This is the basis of photodynamic therapy for treating tumors (Kriska et al., 2002). In plants, PPIX induces apoptotic-like events both at the single cell and population levels in a light-dependent manner (Yao et al., 2004). Surprisingly, ACD2 levels modulate the extent of PCD upon PPIX treatment. Furthermore, light-treated *acd2* protoplasts or PPIX-treated wild-type protoplasts show early mitochondrial membrane potential loss that is important for PCD induction. By contrast, pheophorbide A does not induce PCD, even though it is a precursor of RCC and the proposed substrate of ACD1 (Pruzinska et al., 2003; Yao et al., 2004). Together, our findings suggest the involvement of mitochondria in the *acd2* phenotype. Furthermore, they raise the possibility that molecules other than RCC are substrates for ACD2 and that chlorophyll breakdown is not essential for modulating cell death controlled by ACD2.

In this work, we further characterized the role of ACD2 in cell death control. Here, we focused on ACD2 localization during pathogenesis and PPIX treatment, its effects on pathogen-induced symptoms and bacterial replication, its role in PCD protection in cells that lack chlorophyll, and the early events important for the PCD that it modulates. ACD2 shows dynamic localization during infection, shifting from being mainly chloroplast localized to having a broader distribution that includes mitochondria and cytoplasm. We find that ACD2 overexpression significantly delays the HR and reduces *P. syringae* replication early in the infection process. Strikingly, ACD2 modulates light- and PPIX-induced PCD in root protoplasts, suggesting a role for ACD2 that is independent of chlorophyll breakdown. Finally, ACD2-modulated PCD requires an early mitochondrial oxidative burst. This is followed by chloroplast-produced nitric oxide (NO), mitochondria and chloroplast behavior and morphology changes, and cell death. A plausible scenario is that during infection, ACD2 may bind and/or reduce a porphyrin-related molecule(s) that generates light-dependent reactive oxygen species. These activated molecules may reside in mitochondria and/or chloroplasts and cause an alteration in their behavior that leads to PCD.

RESULTS

ACD2 Localizes to Chloroplasts and Mitochondria during *P. syringae* Infection and PPIX Treatment

Phenotypic characterization of *acd2* mutant plants suggested a possible role for mitochondria in cell death control mediated by ACD2 (Yao et al., 2004). To further investigate the role of ACD2 in cell death control, we immunolocalized ACD2 after cell death induction in ultrathin sections using electron microscopy. As shown in Figure 1A, in healthy leaves, ACD2 was highly localized to chloroplasts, consistent with previous fractionation results (Mach et al., 2001). Almost no immunodecoration of leaf sections was found in *acd2* mutant samples (Figure 1B). ACD2 localization was highly associated with starch grains (~70% of the gold-labeled particles were within starch grains). Much less ACD2 was detected in leaves that were placed in the dark for 24 h (Figure 1H). In these leaves, ACD2 was evenly distributed within chloroplasts, and starch grains were absent (data not shown). Finally, in 35S:ACD2 plants, most of the ACD2 protein also localized to chloroplasts around the starch grains, but there was a dramatic increase in mitochondrial and cytosolic labeling relative to the wild type (Figure 1H). Approximately 50% of the nonchloroplast pool of ACD2 was in mitochondria.

In order to compare ACD2 localization in dead cells, dying cells, and living cells in the same tissue, we infected leaves with *Pma* DG6, an avirulent strain of *P. syringae* pv *maculicola* carrying *avrRpt2*, at 5×10^6 colony-forming units (cfu)/mL. The death of isolated single cells (called HR cells) was observed 18 h after infection (Figure 1C). ACD2 localization was assayed in three types of cells: HR cells, dying cells that were adjacent to HR cells (1st zone), and living cells that were adjacent to 1st zone cells (2nd zone). We found dramatic cell wall shrinkage and collapse of the HR cells. In these cells, most organelles were disrupted and crushed (Figure 1D); very little ACD2 protein was detected. In 1st zone cells, ACD2 was evenly distributed within chloroplasts and was also found in mitochondria and cytosol (Figures 1E and 1F). Supplemental Figure 1 online shows an enlarged view of the mitochondrion in Figure 1F immunodecorated with anti-ACD2 antiserum. Approximately 70% of the nonchloroplast pool of ACD2 in 1st zone cells was in mitochondria (Figure 1H). Most 1st zone cells had PCD features, such as chromatin condensation (Figure 1K) and endonucleolytic cleavage of DNA detected by electron microscopic–terminal deoxynucleotidyl transferase (EM-TUNEL) staining (Figure 1L). These cells had fewer starch grains.

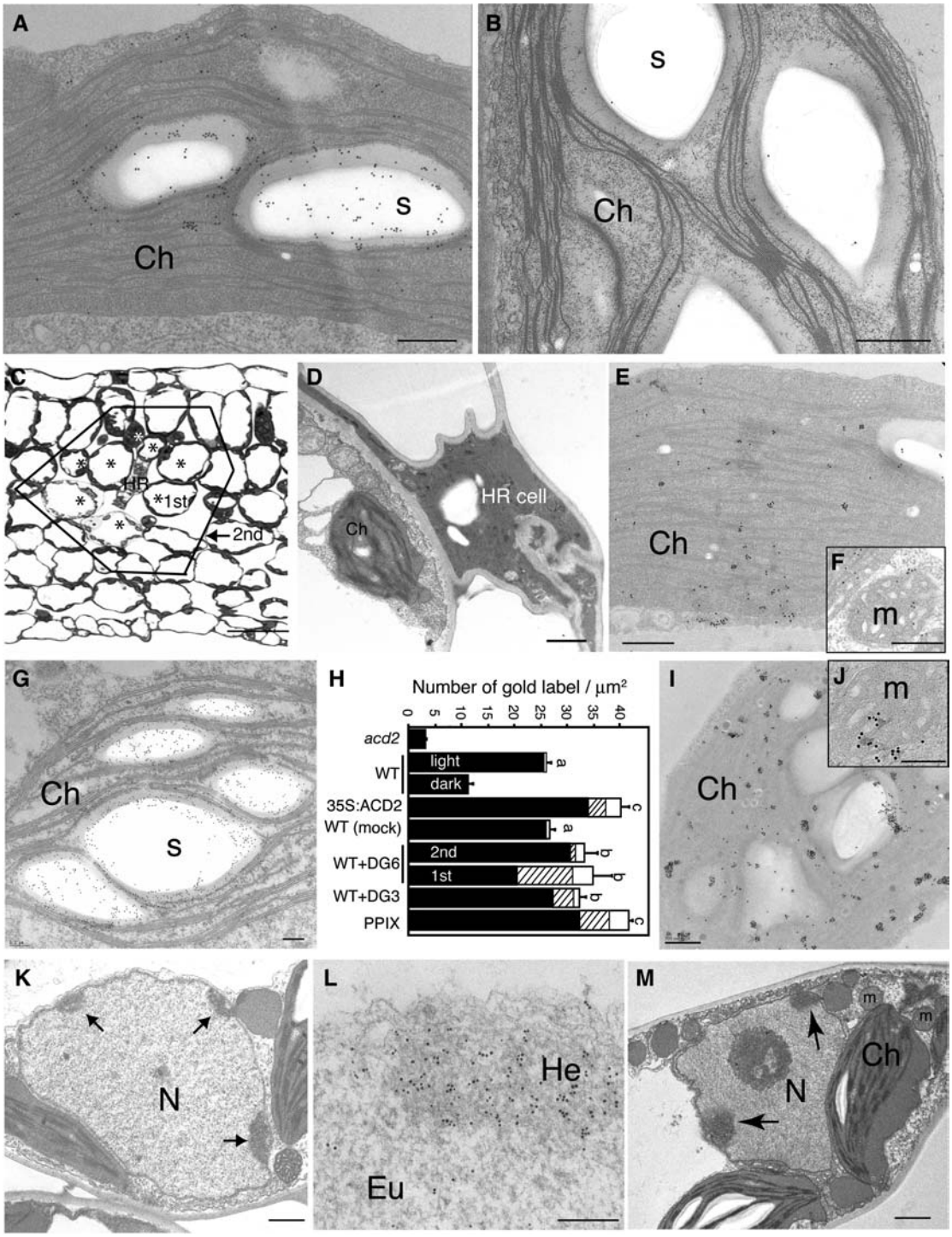

Figure 1. Subcellular Localization of ACD2 in *P. syringae*–Infected Leaves.

(A) and **(B)** ACD2 localization in 18-d-old wild-type **(A)** and *acd2* mutant **(B)** leaves.

(C) Cross section of wild-type leaves after low dose infection of the avirulent *P. syringae* strain DG6 for 18 h. HR indicates a dead HR cell. Asterisks and solid line indicate cells adjacent to the HR cell (1st zone) and cells adjacent to the 1st zone cells (2nd zone), respectively.

(D) Dramatic cell wall shrinkage and cell collapsed in the HR cell.

(E) to **(G)** ACD2 localization after bacterial infection as shown in **(C)**. Note that ACD2 is more evenly distributed within chloroplasts **(E)** and is also found in mitochondria **(F)** in the 1st zone cell. In the 2nd zone cell, ACD2 is highly localized in close association with the starch grains in the chloroplasts **(G)**.

(H) Statistical analysis of the density of gold-labeled ACD2 in chloroplasts (closed bar), mitochondria (hatched bar), and other parts of the cells (mainly

In 2nd zone cells, ACD2 was mainly in chloroplasts, especially around starch grains. However, in these cells, ACD2 localization in mitochondria and cytosol was significantly higher than in untreated or mock-inoculated control leaves (Figures 1G and 1H). Compared with the controls, ACD2 showed dramatically enhanced mitochondria and cytosol localization in the 1st zone cells (Figure 1H). Additionally, the level of ACD2 in 1st and 2nd zone cells was higher than in the mock-inoculated control (Figure 1H).

In dying cells of leaves infected with the congenic virulent pathogen *P. syringae* pv *maculicola* strain DG3, ACD2 localized to both chloroplasts and mitochondria (Figure 1H). These dying cells also showed PCD features, such as chromatin condensation (Figure 1M). Furthermore, PPIX, which also induces PCD, induced altered ACD2 localization and levels (Figures 1H to 1J). Thus, altered localization of ACD2 may be a general feature of dying cells and their close neighbors in an infection zone or from treatments such as PPIX exposure that partially mimic infection.

An early change in mitochondrial function is important for cell death in PPIX-treated wild-type and *acd2* cells and in light-treated *acd2* cells (Yao et al., 2004). Additionally, *acd2* mutant leaves show spreading cell death (Greenberg et al., 1994). Along with the dynamic localization of ACD2, these observations suggest that the effects of ACD2 in protecting cells from PCD could be exerted in chloroplasts and/or mitochondria.

ACD2 Delays Cell Death and Pathogen Growth after Avirulent Pathogen Infection

ACD2 overproduction protects plants from disease symptoms caused by virulent *P. syringae*. However, it does not protect plants from macroscopic cell death due to high dose inoculations of avirulent *P. syringae* (Mach et al., 2001). To test whether ACD2 overexpression affects the HR during low dose infections, we observed localized cell death at different times compared with the wild type in response to infection with 5×10^6 cfu/mL of *P. syringae* carrying *avrRpt2* (strain *Pma* DG6). We counted each infiltrated leaf that showed visible localized cell death over a 48-h time course. As shown in Figure 2A, ACD2 overexpression delayed the appearance of cell death when compared with the wild type. As shown in Figure 1C, we cut three independent leaves in each treatment to make tissue blocks for electron microscopic observations. In each block, 30 cross sections were observed. Strikingly, at 18 h, although no visible cell death was seen in either wild-type or 35S:ACD2 leaves, microscopic single cell death occurred only in wild-type infected leaves.

To determine whether the delay in cell death during infection was accompanied by altered pathogen growth, we monitored *P. syringae* levels at 2 and 3 d after infection. Avirulent *P. syringae* carrying *avrRpt2* (strain *Pma* DG6) showed eightfold reduced levels in 35S:ACD2 plants relative to the wild type 2 d after infection. However, by day 3, bacterial growth was similar in 35S:ACD2 and wild-type plants (Figure 2B). Virulent *P. syringae* strain *Pma* DG3 showed a similar transient reduction in bacterial growth in 35S:ACD2 plants with low dose infection (Figure 2B). These data suggest that ACD2 levels can modulate the onset of the HR and affect the early replication or survival of both virulent and avirulent bacteria.

It seemed possible that ACD2's effects on *P. syringae* growth, the HR, and/or disease symptoms were caused by reducing oxidative stress, which may be caused by photoactivation of phorphyrin-like molecules during infection. Therefore, we tested whether overproduction of the enzyme ascorbate peroxidase in thylakoids (tAPX) could phenocopy the effects of ACD2 overexpression. Plants overexpressing tAPX are known to be oxidative stress tolerant (Murgia et al., 2004). Like ACD2-overexpressing plants, tAPX plants showed a delay in the onset of the HR (data not shown) and reduced symptoms caused by virulent or avirulent infection after 2 and 3 d, respectively (Figure 2C). Additionally, *P. syringae* replication was transiently reduced for both virulent and avirulent *P. syringae* (Figures 2A and 2B). Plants overexpressing both ACD2 and tAPX showed even less cell death during infection than plants individually overexpressing ACD2 or tAPX (Figure 2C). However, only with the avirulent infection was the combined effect of ACD2 and tAPX overexpression significantly greater than overexpression of the individual proteins (Figure 2B, note the growth of *P. syringae* strain DG6 on day 3). These results suggest that some of ACD2's effects that were nonadditive with tAPX could be due to a reduction of oxidative stress, possibly in chloroplasts. However, the additive effects of ACD2 and tAPX on cell death and avirulent pathogen growth 3 d after infection suggest these two proteins also act on distinct processes and/or in distinct cellular locations. Since most ACD2 localized to mitochondria and chloroplasts and tAPX only localized to chloroplasts (Murgia et al., 2004), events in both mitochondria and chloroplasts likely contribute to cell death during infection.

Figure 1. (continued).

cytosol; open bars). Light and dark indicate wild-type plants under 16-h day condition and 24-h dark treatment, respectively. Mock indicates 10 mM $MgSO_4$ control treatment of wild-type plants. In WT+DG6, the 1st and 2nd zone cells were investigated. Approximately 25 cells each in the wild-type controls and 1st and 2nd zones were photographed for statistical analysis of the density of ACD2 localization. Letters indicate that values of total density of gold-labeled ACD2 are different using Fisher's protected least significant difference (PLSD), a post hoc multiple *t* test ($P < 0.05$). Error bars indicate standard error. In WT+DG3, 21-d-old leaves 48 h after bacterial infiltration (1×10^6 cfu/mL) were investigated. PPIX means that 20-d-old leaves were treated with 50 μM PPIX for 48 h.

(I) and **(J)** ACD2 localization in PPIX-treated leaves.

(K) and **(L)** Chromatin condensation **(K)** and EM-TUNEL **(L)** in *P. syringae* DG6-infected leaves.

(M) Chromatin condensation in a cell infiltrated with virulent *P. syringae* DG3 at 1×10^6 cfu/mL for 48 h. These experiments were repeated three times with similar results.

Ch, chloroplast; Eu, euchromatin; He, heterochromatin; m, mitochondrion; N, nucleus; s, starch grain. Bars = 200 nm in **(A)**, **(B)**, **(E)** to **(G)**, **(I)**, **(J)**, and **(L)**, 1 μm in **(D)**, **(K)**, and **(M)**, and 50 μm in **(C)**.

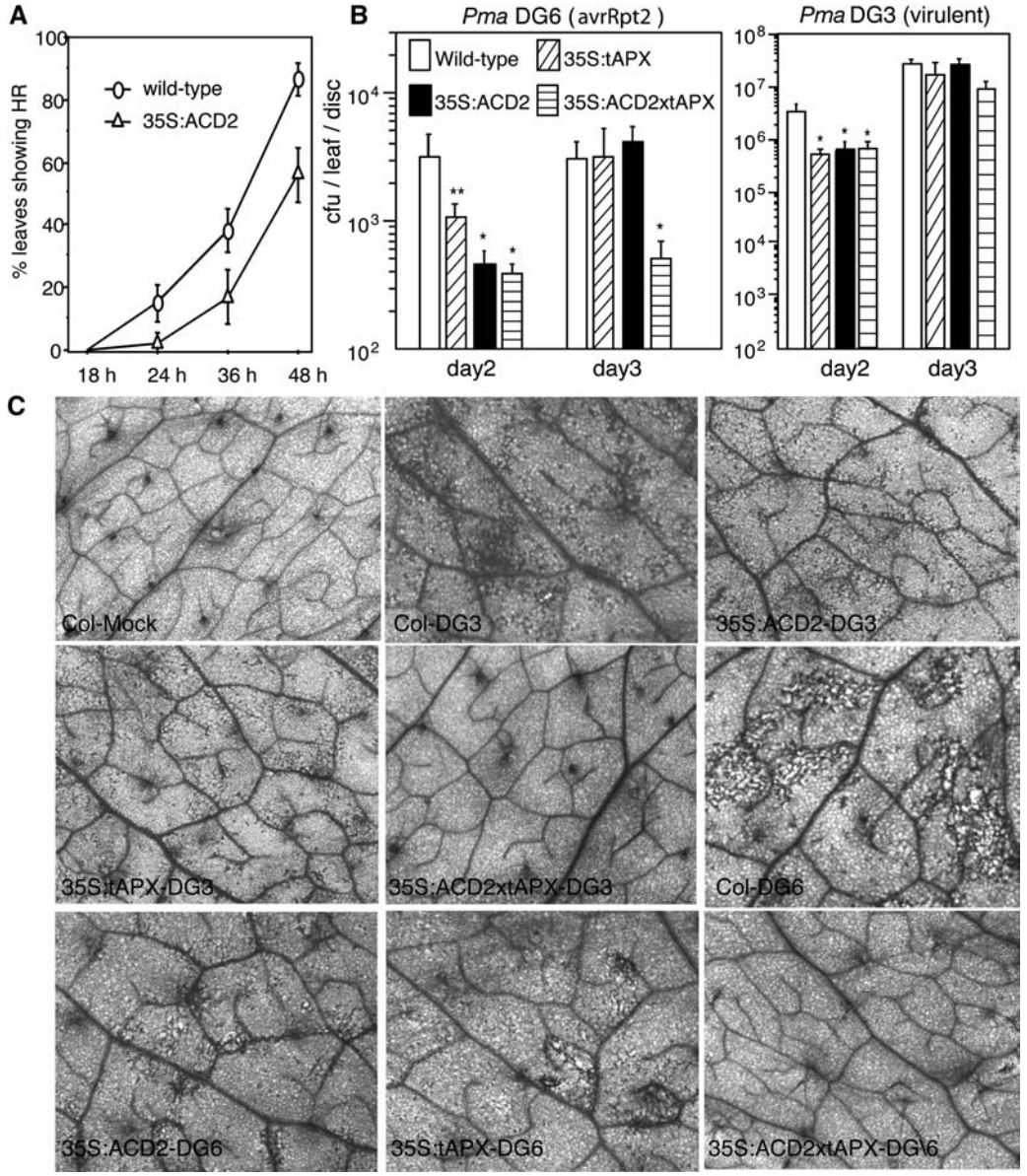

Figure 2. Pathogen Symptoms and Growth in ACD2- and tAPX-Overexpressing Leaves.

(A) Cell death phenotype after infection by *P. syringae* carrying *avrRpt2* at $OD_{600} = 0.005$. Thirty-nine leaves for each genotype were infiltrated in two independent experiments, and the HR was scored as any visible brown spot larger than 2 mm.

(B) Growth of *avrRpt2*-containing strain *Pma* DG6 or the congenic virulent strain *Pma* DG3 in the indicated genotypes after infection at $OD_{600} = 0.0001$. Nine and six leaf punches were used to monitor growth on days 2 and 3, respectively. One asterisk indicates $P < 0.05$, and two asterisks indicates $P < 0.09$ using Fisher's PLSD. Error bars in **(A)** and **(B)** indicate standard error.

(C) Trypan blue staining to visualize cell death on the indicated days in leaf tissue after infection with *Pma* DG3 (virulent) or *Pma* DG6 (*avrRpt2*) using the dose indicated in **(B)**. Mock treatment was with 10 mM $MgSO_4$. These experiments were repeated twice with similar results.

ACD2 Has a Function Independent of Chlorophyll Catabolism

Previously, we showed that the amount of PCD during *P. syringae* infection and PPIX-treated leaf tissue and protoplasts correlates with the amount of ACD2 (Mach et al., 2001; Yao et al., 2004). Because ACD2 can catabolize chlorophyll in vitro (Wüthrich et al., 2000), chlorophyll catabolite levels could be responsible for different PCD levels we observed. Does ACD2 function depend on chlorophyll catabolism? To answer this question, we isolated protoplasts from *acd2* mutant, wild-type, and ACD2-overexpressing roots, a tissue that lacks chlorophyll, and treated them with or without PPIX in the presence or absence of light. As shown in Figure 3B, *acd2* root protoplasts

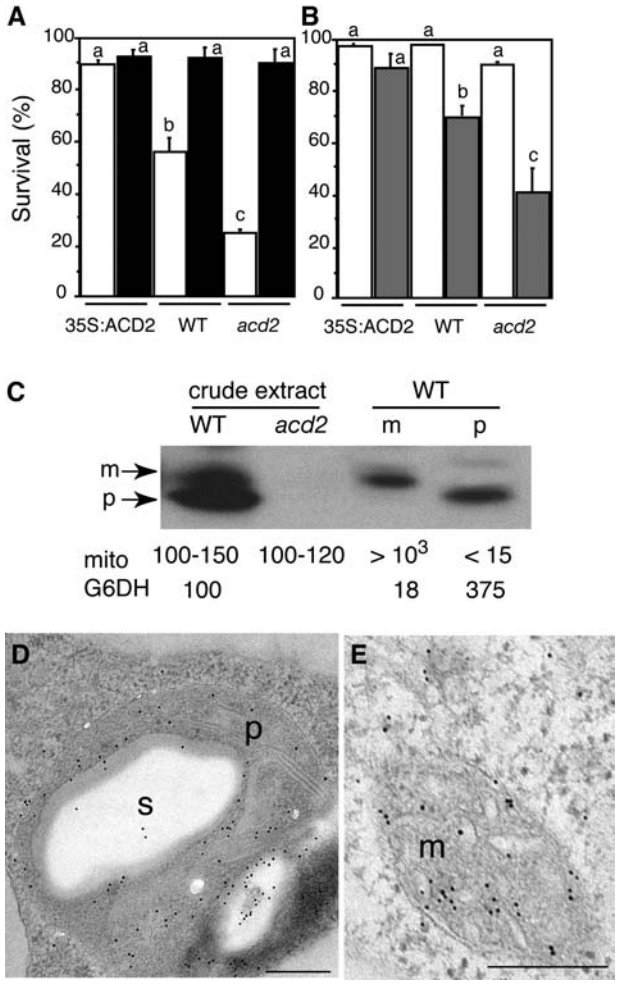

Figure 3. ACD2 Localization and Function in Root Tissues.

(A) *acd2* root protoplasts showed cell death after incubation in the light. Protoplasts from 26-d-old 35S:ACD2, wild-type, and *acd2* roots were cultured for 24 h. Open and closed bars indicate incubation in the light and dark, respectively. Standard errors are shown ($n = 3$). Letters indicate different values using *t* test ($P < 0.03$). Percentage of surviving cells in each population was determined by fluorescein diacetate staining.

(B) ACD2 modulation of cell survival in root protoplasts in response to PPIX. Protoplasts from 26-d-old 35:ACD2, wild-type, and *acd2* mutant roots were treated with (shaded bars) or without (open bars) 20 μM PPIX for 4 h in the light. Standard errors are shown ($n = 3$). Letters indicate different values using Fisher's PLSD test ($P < 0.03$).

(C) Protein gel blot analysis of *acd2* mutant and wild-type root tissues with anti-ACD2 antiserum. Root tissues were partitioned into mitochondria (m) and plastid (p) fractions. m, mitochondrial form of ACD2; p, plastid form of ACD2; mito, mitochondria/microliter; G6DH, plastid marker enzyme activities relative to the levels in crude extracts.

(D) and **(E)** ACD2 localization to plastids **(D)** and mitochondrion **(E)** in 26-d-old wild-type root tissues. These experiments were repeated three times with similar results. m, mitochondrion; p, plastid; s, starch grain. Bars = 200 nm.

showed more PPIX-induced cell death than the wild type. Upon prolonged incubation in the light (without PPIX), *acd2* root protoplasts also showed more cell death than the wild type (Figure 3A). ACD2-overexpressing protoplasts showed no cell death in the light with or without PPIX treatment (Figures 3A and 3B). Thus, root protoplasts incubated in the presence of light from the three genotypes showed similar sensitivity to the PPIX-induced leaf protoplast PCD (Yao et al., 2004): *acd2* was more sensitive to PPIX than the wild type and the wild type was more sensitive than the ACD2-overexpressing cells. These data indicate that chlorophyll is not necessary for ACD2's effect on PCD induction.

Roots had lower ACD2 levels than leaves on a fresh weight basis (data not shown). To address the subcellular localization of ACD2 in roots, we purified plastids and mitochondria from 26-d-old soil-grown root tissue and analyzed protein levels in the organelles by protein gel blot analysis. Plastid enrichment was confirmed by measuring the plastid-specific marker glucose 6-phosphate dehydrogenase (Journet and Douce, 1985). Mitochondria enrichment was confirmed with the mitochondrial-specific dye MitoTracker Red CMXRos. ACD2 protein was substantially enriched in plastids and mitochondria in roots. The two organellar forms migrated at slightly different sizes, similar to the distribution of ACD2 in 7-d-old seedlings (Figure 3C). Immunoelectron microscopy confirmed that ACD2 localized to both plastids and mitochondria in wild-type roots (Figures 3D and 3E). Given the dual localization of ACD2, it is possible that the mitochondrial and/or chloroplast forms confer an anti-PCD function in roots.

Dynamic Mitochondrial and Chloroplast Changes Occur during Light- and PPIX-Induced PCD

Mitochondria are highly dynamic organelles; their morphology and motility is related to their energy status (Bereiter-Hahn and Vöth, 1994). In animal cells, many apoptosis-related proteins reside at the mitochondrial membrane and control mitochondrial dysfunction (Bernardi et al., 2001). However the relationship between mitochondrial dysfunction and mitochondrial morphology changes remains unclear. Logan and Leaver (2000) have suggested that under normal conditions, plant mitochondria localize around chloroplasts due to oxygen and carbon dioxide gradients, which establish metabolite interchange between the two. We examined the positions of mitochondria and chloroplasts in ultrathin sections and by confocal microscopy. We found that in 40 cells, 315 of 351 mitochondria (90%) were next to chloroplasts. To test if this was true for other organelles, we also examined the positions of peroxisomes. We found that only 61 of 220 peroxisomes (28%) were near chloroplasts. This suggests there may be a specific functional link between mitochondria and chloroplasts.

Alterations in organellar position or shape during cell death induction could indicate their functional alteration. We sought to monitor mitochondrial and chloroplast behavior in real time during PCD induction to see if any behaviors might be correlated with or causal to the PCD process modulated by ACD2. To facilitate the monitoring of organelle behavior in real time, we used the in vivo marker green fluorescent protein (GFP) that was

targeted to mitochondria (β-ATPase-GFP). We also used chloroplast autofluorescence to visualize chloroplast morphology and movements.

Protoplasts isolated from wild-type and *acd2* mutant leaf tissues that expressed GFP in mitochondria were observed by confocal and time-lapse microscopy. In wild-type protoplasts, mitochondria and chloroplasts were often restricted to a narrow band of cytoplasm against the plasma membrane, and mitochondria were evenly distributed around the chloroplasts after incubation for 4.5 h in the light (Figure 4A). However, in light-treated *acd2* and PPIX-treated wild-type protoplasts, the position of mitochondria changed after 4 to 5 h of treatment. In both cases, mitochondria became round in shape, irregularly clumped or clustered surrounding chloroplasts, or aggregated in other places within the cytoplasm (Figures 4B and 4C). In wild-type cells, chloroplasts appeared crescent-shaped, whereas the induction of cell death in *acd2* or in the PPIX-treated wild type caused chloroplasts to appear more evenly rounded. In addition, chloroplasts also showed alteration of their positions (from being close to the plasma membrane to being distributed evenly within the cytoplasm) in PPIX-treated wild-type protoplasts when compared with control protoplasts (Figure 4C). Using electron microscopy observations, we saw no evidence for organelle rupture at this time (data not shown). Similar results were obtained with the 20 or more individual protoplasts observed for each treatment. In addition, the observed cells were still alive, as they stained positive with fluorescein diacetate. We also noted that there were similar numbers of chloroplasts in wild-type and *acd2* plants (data not shown).

In the course of observing organelle movements, we also followed vacuole behavior and the overall shape of the cells. Vacuoles were evident as large purple areas due to the presence of soluble pigments. The appearance of the vacuoles did not change during the period when chloroplast and mitochondrial alterations were seen. However, 1 to 2 h later, there was a sudden reduction in the purple color and loss of the round shape of the cells (data not shown). We interpreted this as vacuolar rupture and cell death. Cells in this state did not stain with fluorescein diacetate. The dynamic movement of mitochondria and chloroplasts preceded cell death occurrence by 1 to 2 h, indicating that both organellar functions were likely altered.

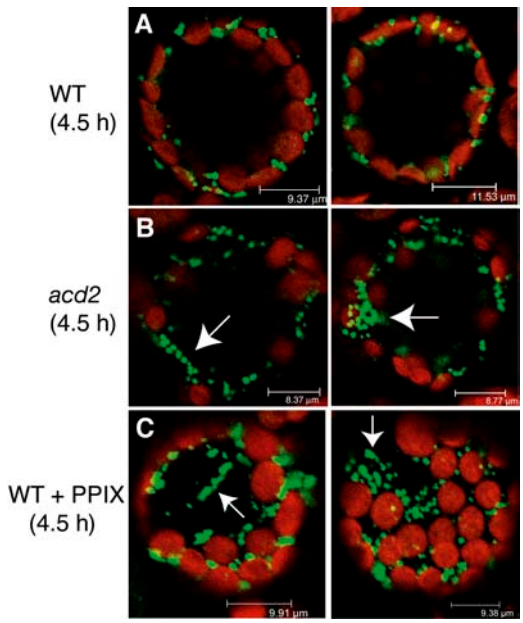

Figure 4. Dynamic Mitochondrial and Chloroplast Movement during Light- and PPIX-Induced *acd2* and Wild-Type Protoplast Cell Death.

Confocal images of mesophyll cells of wild-type and *acd2* mutant protoplasts treated with or without 10 μM PPIX under light. Green signals indicate GFP targeted to mitochondria. Red signals indicate chlorophyll autofluorescence. Note that mitochondria are often positioned around chloroplasts that are near the plasma membrane in the wild type **(A)**. However, in light/PPIX-treated *acd2* **(B)** and wild-type **(C)** protoplasts, mitochondria become irregularly clumped around chloroplasts or distributed in other parts of the cytoplasm (arrows). Also, chloroplasts became round in shape, and most of them were not near the plasma membrane. This experiment was repeated three times with similar results.

Mitochondrial-Derived H_2O_2 Is Essential for the *acd2* Phenotype and PPIX-Induced Cell Death

Previously, mitochondrial membrane potential disruption was observed in light-treated *acd2* and PPIX-treated *acd2* and wild-type protoplasts (Yao et al., 2004). As described above, the behaviors of mitochondria and chloroplasts also dramatically changed during cell death induction. We further examined the reactive oxygen species (ROS) status in organelles to ask whether ROS are involved in cell death events, where ROS are generated, and whether ROS production precedes organelle changes.

We used CM-H_2DCFDA (DCF), a probe for intracellular hydrogen peroxide (H_2O_2), to monitor H_2O_2 production by laser scanning confocal microscopy. We double stained protoplasts with MitoTracker Red CMXRos to simultaneously mark mitochondria. First, we exposed wild-type and *acd2* protoplasts to light for various times. We found that as early as 1.5 h, the *acd2* protoplasts exhibited dramatic increases in DCF fluorescence that colocalized with mitochondria adjacent to chloroplasts (Figure 5B). By contrast, there was no detectable DCF signal in wild-type cells exposed to 4 h of light (Figure 5A). After 3.5 h of light treatment, *acd2* showed large DCF-stained regions that colocalized with mitochondria. The diffused CMXRos staining indicates that mitochondrial function decreased. At this time, chloroplast membranes also stained with DCF (Figure 5C). *N*-acetyl-LL-cysteine (NAC), a free radical scavenger, completely depleted the DCF signals (Figure 5D) and also partially prevented light-induced *acd2* cell death (Figure 6B).

To disrupt chloroplast accumulation of H_2O_2, we crossed *acd2* to 35S:tAPX (Murgia et al., 2004). As shown in Figures 5E and 6B, these protoplasts had reduced H_2O_2 accumulation in chloroplasts, but their mitochondrial DCF signals and light-induced cell death were not significantly affected. Thus, chloroplast-localized H_2O_2 accumulation was not causal to PCD of *acd2*.

As with light-treated *acd2* protoplasts, PPIX-treated wild-type protoplasts showed rapid ROS accumulation, within 2 h of treatment, in mitochondria (Figure 5F). PPIX-induced ROS accumulation and cell death were also partially suppressed in

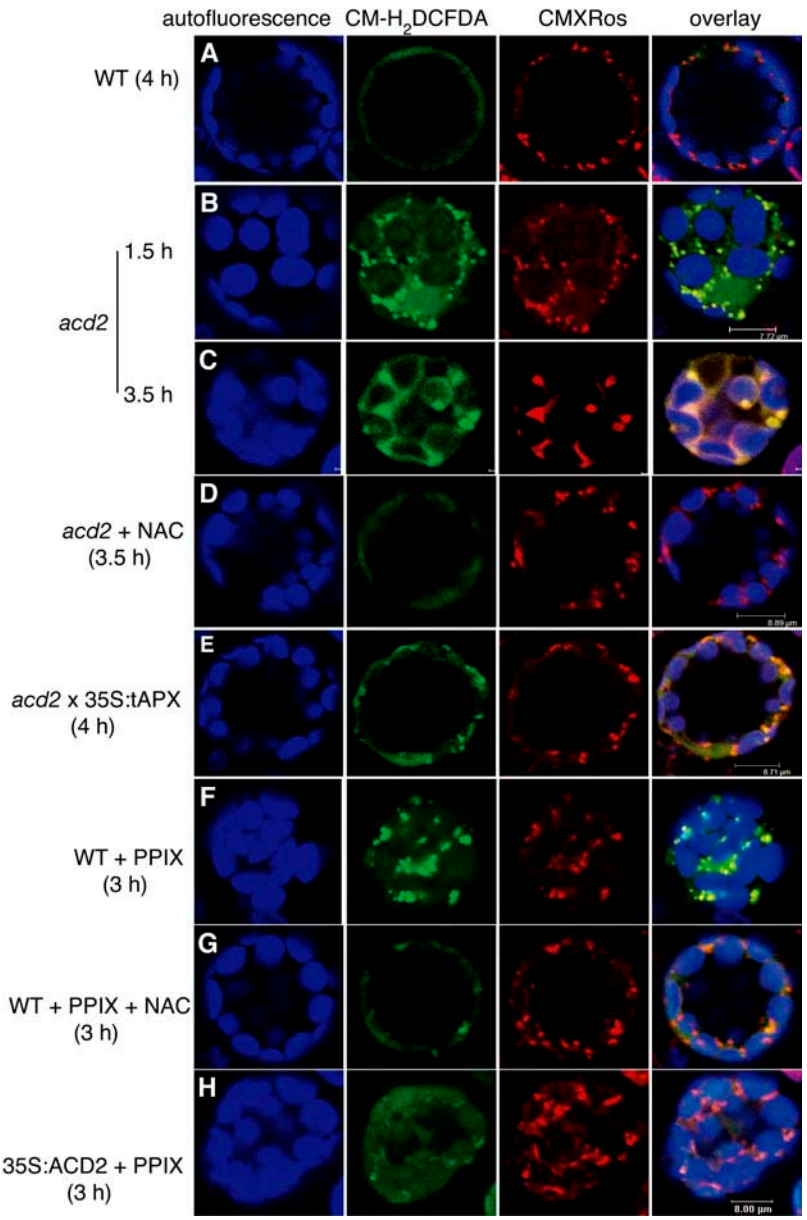

Figure 5. ROS Production in *acd2* and PPIX-Treated Protoplasts.

Protoplasts from 18-d-old wild-type, *acd2* mutant, *acd2* × 35S:tAPX, and 35S:ACD2 leaves were treated with or without 10 μM PPIX under light and double-stained with CM-H_2DCFDA (green) and CMXRos (red). Images were observed by laser scanning confocal microscopy. Chloroplast autofluorescence (blue) was excited at 488 nm and visualized at 738 to 793 nm. This experiment was repeated three times with similar results.

(A) A wild-type control cell. Note that there were no detectable green signals after staining with CM-H_2DCFDA.

(B) to **(D)** *acd2* protoplasts were treated with or without 10 μg/mL NAC for 3.5 h. Note that the localization of the CM-H_2DCFDA signals matched that of the CMXRos signals after 1.5 h. After 3.5 h, green signals were also found in the outer membrane of chloroplasts **(C)** and were significantly decreased by the addition of NAC **(D)**.

(E) A cell homozygous for *acd2* and 35S:tAPX.

(F) and **(G)** Wild-type protoplasts were treated with PPIX or PPIX + NAC for 3 h.

(H) A 35S:ACD2 cell treated with PPIX for 3 h.

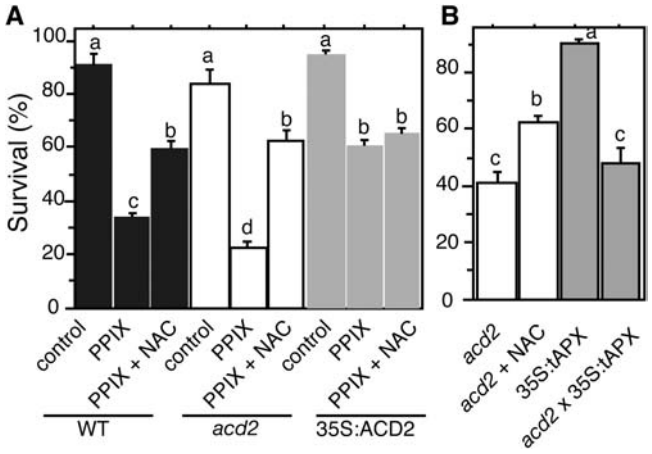

Figure 6. Inhibition of PPIX- and Light-Induced Protoplast Cell Death by NAC.

(A) Protoplasts from 18-d-old wild-type, *acd2* mutant, and 35S:ACD2 leaves were treated with 10 μM PPIX in the absence or presence NAC (10 μg/mL) for 8 h in the light. Control treatment was with 0.1% DMSO (the solvent for PPIX).

(B) Protoplasts from 19-d-old *acd2* mutant, 35S:tAPX, and *acd2* × 35S:tAPX leaves were treated with or without 10 μg/mL NAC for 14 h under light.

Standard errors in **(A)** and **(B)** are shown ($n = 3$). Letters indicate different values using Fisher's PLSD test ($P < 0.04$). Percentage of survival cells in population was determined by fluorescein diacetate staining. These experiments were repeated three times with similar results.

the presence of NAC (Figures 5G and 6A). Interestingly, ACD2-overexpressing protoplasts showed partially decreased DCF signals after PPIX treatment (Figure 5H). However, NAC did not increase the survival of ACD2-overexpressing protoplasts after PPIX treatment (Figure 6A). We also tested 35S:tAPX plants with PPIX treatment. These plants were unaltered in their DCF signals from mitochondria and showed only a modest affect on enhancing protoplast survival compared with ACD2-overexpressing protoplasts (data not shown). Root protoplasts also showed a PPIX-induced mitochondrial oxidative burst that was suppressed by NAC (Figure 7). This suggests that PPIX affects leaf and root cells similarly.

To more precisely localize H_2O_2, we did ultrastructural analysis using a cytochemical assay based on the reaction of H_2O_2 with $CeCl_3$. In *acd2* mutant leaves, strong H_2O_2 production (recognized as electron-dense, insoluble precipitates of cerium perhydroxides) was found along the chloroplast and mitochondrial outer membranes in the leaf tissue undergoing spontaneous cell death (Figures 8A and 8B). In PPIX-infiltrated wild-type plants, H_2O_2 localized to mitochondria (Figure 8E). Low levels of cerium deposits were also found in starch grains of the chloroplast (Figure 8F). No cerium deposits were found in wild-type control plants (Figures 8C and 8D).

Taken together, ROS, especially mitochondrion-derived H_2O_2, played an important role in *acd2* and PPIX-induced cell death. Although an increase in the chloroplast antioxidant level delayed chloroplast ROS production, it seems chloroplasts are not the sites of H_2O_2 production that are causal to cell death in light-treated *acd2*. We also noted that based on a time-course analysis of PPIX-treated wild-type protoplasts, mitochondrial ROS production preceded mitochondrial morphology changes, such as loss of mitochondrial cristae structures, swelling, and becoming rounded (Figure 8H). In control protoplasts, mitochondria appeared elongated (Figure 8G).

NO Localizes to Subregions of the Chloroplast during Cell Death Induction

The gas NO, which is a well-characterized signaling molecule in mammals, is also a signal in plants that is involved in disease resistance pathways (Clarke et al., 2000; Delledonne et al., 1998). To investigate where and when NO is produced and whether NO is causal to PCD, we applied 4-amino-5-methylamino-2′,7′-difluorofluorescein (DAF-FM) diacetate to observe NO accumulation in PPIX-induced PCD.

In wild-type protoplasts, NO did not accumulate after 4 h of incubation in the light (Figure 9A). However, NO was produced in subregions of chloroplasts in PPIX- treated protoplasts. Its accumulation was later than H_2O_2 production (Figure 9B).

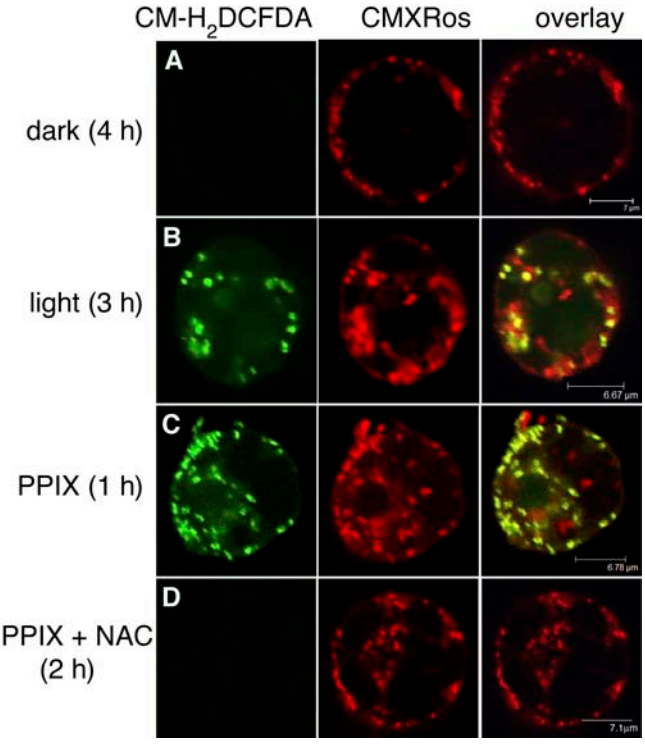

Figure 7. ROS Production in Light- and PPIX-Treated Root Protoplasts.

Protoplasts from 28-d-old wild-type roots were treated with or without 20 μM PPIX or PPIX + NAC (10 μg/mL) for the indicated times in the dark or light and then double-stained with CM-H_2DCFDA (green) and CMXRos (red). Images were observed by laser scanning confocal microscopy.

(A) and **(B)** Cells were cultured in the dark **(A)** and light **(B)**. Note there were no detectable green signals in the dark treatment, whereas ROS accumulation was found after light treatment.

(C) and **(D)** Root cells were treated with PPIX or PPIX + NAC. Note dramatic ROS production was found in mitochondria after PPIX treatment **(C)** and completely depleted when NAC was added **(D)**.

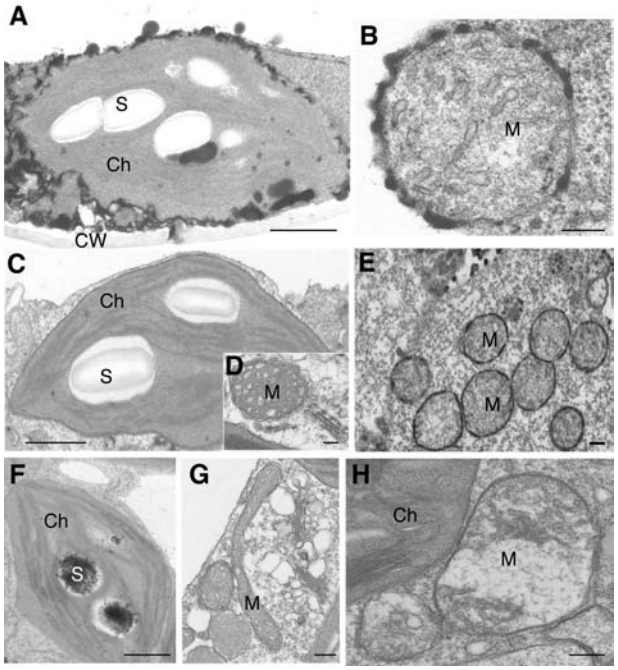

Figure 8. Cytochemical Localization of H_2O_2 Using Cerium Chloride Staining of *acd2* Mutant and PPIX-Treated Wild-Type Leaves.

(A) and **(B)** Twenty-day-old *acd2* leaves with some spontaneous cell death were used. Note electron-dense deposits of cerium perhydroxidase, indicative of the presence of H_2O_2 in the chloroplast **(A)** and mitochondrial **(B)** outer membranes. The chloroplast and mitochondrion were structurally intact.

(C) and **(D)** Wild-type control leaves stained with cerium chloride.

(E) and **(F)** Wild-type leaves infiltrated with 50 μM PPIX for 24 h. Note the presence of H_2O_2 in the outer membranes of clustered mitochondria **(E)** and in starch grains of chloroplast **(F)** in cells adjacent to those that died.

(G) and **(H)** Protoplasts from 18-d-old wild-type leaves were treated with **(H)** or without **(G)** 10 μM PPIX for 5 h in the light and then fixed to make regular electron microscopy samples. Note that mitochondria became swollen and round in shape in a PPIX-treated cell **(H)** when compared with a control cell **(G)**.

These experiments were repeated three times with similar results. Ch, chloroplast; CW, cell wall; M, mitochondrion; S, starch grain. Bars = 1 μm in **(A)**, **(C)**, and **(F)** and 200 nm in **(B)**, **(D)**, **(E)**, **(G)**, and **(H)**.

PPIX-treated wild-type protoplasts challenged in the presence of cPTIO, a NO scavenging compound, showed markedly reduced fluorescence in subregions of chloroplasts (Figure 9C). cPTIO also slightly decreased PPIX-induced cell death (data not shown). Interestingly, very little NO accumulated in light-treated *acd2* protoplasts during the time course. Furthermore, ACD2 overproduction did not alter the timing or extent of NO production. Thus, compared with the early and significant role of mitochondrial ROS, chloroplast NO played only a small role in cell death induction.

ACD2 Overexpression Confers Herbicide Tolerance

Previously, we found ACD2-overexpressing plants to have partially decreased mitochondrial membrane potential loss and cell death upon PPIX treatment (Yao et al., 2004). PPIX production might function as an endogenous cell death trigger. To test whether ACD2 function is related to PPIX accumulation and/or H_2O_2 production, we employed two herbicides with different modes of action: oxyfluorfen and paraquat. The diphenyl ether herbicide oxyfluorfen inhibits protoporphyrinogen oxidase; the accumulated protoporphyrinogen IX leaks form the plastid and then is converted to PPIX by herbicide-insensitive enzymes in the cytoplasm. This mode of action of oxyfluorfen was confirmed in a series of experiments (Jacobs and Jacobs, 1993; Lee et al., 1993; Matsumoto et al., 1999). Paraquat blocks the electron transport chain during photosynthesis in chloroplasts, causing the production of O_2^- (Bus et al., 1974; Murgia et al., 2004).

We isolated protoplasts from wild-type, *acd2*, and 35S:ACD2 leaves and treated them with oxyfluorfen and paraquat for various times. *acd2* was more sensitive to 10 μM oxyfluorfen than the wild type, whereas ACD2-overexpressing protoplasts showed reduced cell death (Figure 10A). This supports our previous finding that ACD2 levels modulate sensitivity to PPIX treatment (Yao et al., 2004). When treated with 1 μM paraquat, *acd2* mutant protoplasts showed more cell death than the wild type. However, ACD2-overexpressing protoplasts failed to protect cells from paraquat treatment (Figure 10B). Thus, ROS might not be directly related to ACD2 function, but rather might be a consequence of PCD activation in *acd2* mutant plants.

DISCUSSION

Light is essential for the autotrophic lifestyle of plants. However, with the ability to benefit from light comes the need to also control molecules subject to photooxidation caused by light exposure. These molecules can potentially activate excessive PCD and compromise plant fitness. The requirement for light for many PCDs in plants (Greenberg, 1997) raises the possibility that photooxidation of specific molecules contributes to the initiation and/or amplification of PCD, for example, during pathogen infection.

ACD2 is a plant-specific chloroplast protein that modulates cell death during *P. syringae* infection or treatment with PPIX in the light. Without ACD2, plants show spontaneous light-dependent PCD that requires protein synthesis (Asai et al., 2000; Mach et al., 2001; Yao et al., 2004). *acd2* mutants also show spreading cell death upon infection (Greenberg et al., 1994). Overproduction of ACD2 reduces the amount of PCD during infection (Mach et al., 2001; this work). In vitro, ACD2 can perform one of the steps in the breakdown of chlorophyll (Wüthrich et al., 2000). This led to the hypothesis that chlorophyll catabolites modulate PCD during infection and possibly other kinds of stress (Mach et al., 2001). While chlorophyll catabolites might mediate PCD, ACD2 can protect cells from light and PPIX (in the presence of light) even when no chlorophyll is present. Furthermore, during pathogenesis or when ACD2 is overexpressed, the distribution of ACD2 changes, causing significant increases in the amount of ACD2 that localizes to mitochondria and cytosol. Early after *acd2* exposure to light or wild type exposure to PPIX, a mitochondrial oxidative burst occurs that is essential for full levels of subsequent cell death. Together, our findings strongly suggest that ACD2's role in cell death control is at least partially chlorophyll

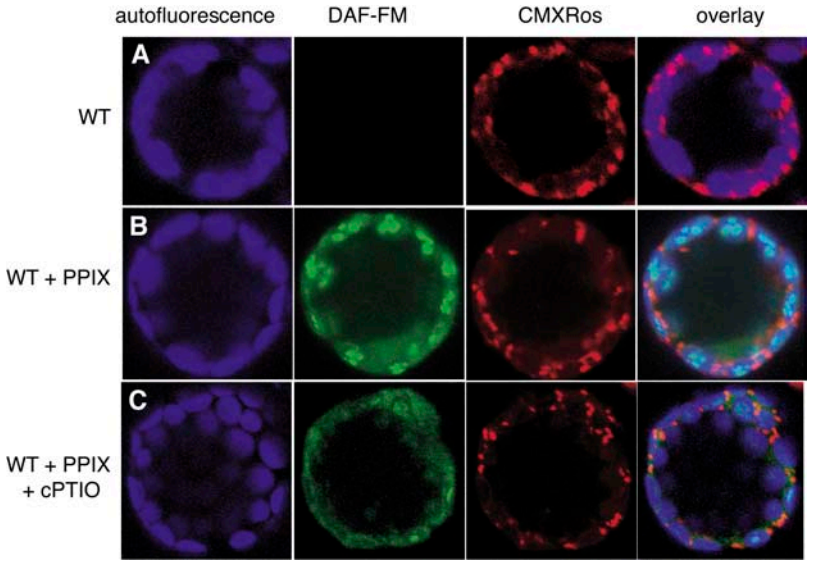

Figure 9. NO Accumulation Localized to Subregions of Chloroplasts in PPIX-Induced Cell Death.

Protoplasts from 18-d-old wild-type leaves were treated with 10 μM PPIX or PPIX + cPTIO (25 μM) for 4 h in the light. Protoplasts were double-stained with DAF-FM (green) and CMXRos (red) and observed by laser scanning confocal microscopy. This experiment was repeated three times with similar results.

independent and involves protecting mitochondria. It seems likely that ACD2's role in plants is to protect them from PPIX and/or similar molecules to prevent excessive cell death.

ACD2 Localization Changes

In vitro, the reduction of RCC can be demonstrated only under anoxic conditions. The relevance of this finding for chlorophyll breakdown in vivo is not clear (Rodoni et al., 1997; Wüthrich et al., 2000). RCCR/ACD2 is a soluble constitutive component of plastids or chloroplasts localized in stroma (Matile et al., 1999). ACD2 (RCCR) contains a predicted chloroplast transit peptide and localizes to chloroplasts in mature plant leaves. However, in young seedlings and root tissues, ACD2 has dual localization in both chloroplasts (or plastids) and mitochondria (Mach et al., 2001). Furthermore, during cell death induction, such as that caused by bacterial infection or PPIX treatment, ACD2 protein localization changes from being mostly in chloroplasts to being targeted to chloroplasts, mitochondria, and cytosol. The cytosolic pool may reflect incomplete targeting of ACD2 to organelles. The mechanism underlying the dual organelle localization of the ACD2 protein is unclear. The chloroplasts/plastid and mitochondria forms of ACD2 are different sizes. This could occur through use of different start sites and/or use of different cleavage sites upon import into the different organelles.

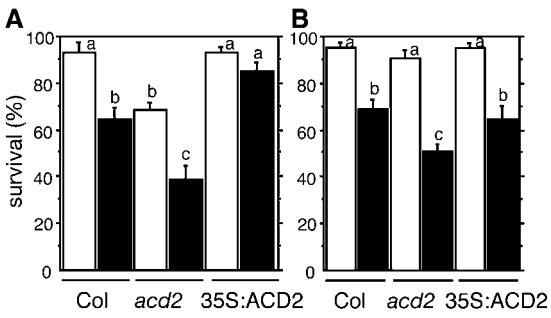

Figure 10. Herbicide-Induced Cell Death.

(A) Protoplasts from 18-d-old wild-type, *acd2* mutant, and 35S:ACD2 plants were treated with 10 μM oxyfluorfen (closed bars) or without (open bars) for 14 h under light. Letters indicate different values using Fisher's PLSD test ($P < 0.02$).

(B) Protoplasts from 18-d-old wild-type, *acd2* mutant, and 35S:ACD2 plants were treated with 1 μM paraquat (closed bars) or without (open bars) for 5 h under light. Letters indicate different values using Fisher's PLSD test ($P < 0.04$).

Error bars indicate standard error. These experiments were repeated three times with similar results.

In plants, several proteins are targeted to both plastids and mitochondria (Watanabe et al., 2001; Chew et al., 2003). Some mitochondrial proteins show an altered degree of import upon stress induction caused by drought or herbicide treatment (Taylor et al., 2003). ACD2 localization could be regulated in response to localized oxidative stress signals. One possibility is that ACD2 substrates may reside in both chloroplasts and mitochondria.

ACD2 is highly associated with stroma storage starch grains in chloroplasts. After dark treatment, much less ACD2 was detected in chloroplasts lacking starch grains. In leaves infected with avirulent bacteria, the amount of ACD2 protein moderately increased in the 1st and 2nd zone cells. Previously, we reported no significant difference in ACD2 protein levels during *P. syringae* infection (Mach et al., 2001). This may be because protein quantitation by protein gel blot analysis diluted local information in the infection zone or because, here, we used a lower dose of

bacteria than was previously employed (Mach et al., 2001). Concomitant with changes in the levels and distribution changes of ACD2, there was a loss of starch grains in the 1st zone cells. Within chloroplasts, ACD2 changed from being associated with starch grains to being distributed throughout the organelle. Starch breakdown in the light is not a normal feature of wild-type plants. However, its breakdown in the light can be triggered by a combination of metabolic signals and redox changes in the chloroplast stroma (Walters et al., 2004). This suggests there may be a localized signal(s) in 1st zone cells during the HR that causes starch breakdown.

ACD2 Function in Disease Resistance

Overexpression of ACD2 delayed cell death and the replication of both virulent and avirulent *P. syringae* during low dose infections. The plant cells that died in the infection zone of these two types of infection both showed apoptotic-like morphologies. The initial disease resistance that extra ACD2 afforded could be a direct effect of the delay in cell death. This would imply that cell death during the HR (or during virulent infection) does not protect plants against *P. syringae* infection as has been reported for viral infection during the HR (Hatsugai et al., 2004). We did not detect an increase in the expression of the defense-related gene *PATHOGENESIS-RELATED1* in the ACD2 overexpression plants (H.W. Jung and J.T. Greenberg, unpublished data), suggesting the major defense pathway that limits *P. syringae* replication (salicylic acid–mediated defenses) was not constitutively activated. However, we have not ruled out that ACD2 might prime a faster defense response upon infection and/or confer disease resistance through a mechanism unrelated to cell death. Manipulation of chlorophyllase levels affected the activation of defense pathways during infection (Kariola et al., 2005). Interestingly, we found that tAPX plants also had reduced bacterial replication and reduced visible HR and disease symptoms. This suggests that while redox signals help activate defenses (Mou et al., 2003), they also contribute to disease susceptibility.

ACD2 Biochemical Function

If ACD2 does not solely function to break down chlorophyll, what might be its function? To catalyze the reduction of RCC, ACD2 must bind to RCC. Given that in vivo ACD2 can protect cells from the effects of PPIX, it is possible that ACD2 directly binds to PPIX and/or other similar molecules that may accumulate or be liberated from bound forms during infection. Such binding may prevent the photooxidation by light of poryphyrin, tetraphyrrole, or similar molecules. It is also possible that ACD2 not only binds but also reduces one or more molecules that are normally photoreactive. In this context, it is not immediately clear what the role of ACD2 is in roots, a tissue that normally is not exposed to much light. Possibly some ACD2 substrates can be activated to cause cell death without light, or ACD2 may be present in roots to protect them from the small amount of light that penetrates soil. We note that root protoplasts were generally more sensitive to light than leaf protoplasts. Furthermore, root cells have less ACD2 than leaf cells (Mach et al., 2001). The level of ACD2 in root cells paralleled their sensitivity to light, suggesting that an endogenous PCD inducer(s) that is an ACD2 substrate is present in roots.

Protoporphyrinogen oxidase (Protox) is the final enzyme in the pathway of chlorophyll and heme biosynthesis. Thus, it plays a role in distributing PPIX to both pathways. Two isoenzymes, a plastidic and a mitochondrial form, have been reported in plants (Lermontova et al., 1997; Watanabe et al., 2001). This information suggests that PPIX could be produced or accumulated in both chloroplasts and mitochondria and thus might be related to ACD2 function. In fact, upon PPIX treatment, we found that ACD2 levels modulate cell death in both leaf and root tissues. These data indicate that although ACD2 may function in the chlorophyll breakdown pathway, it has a function independent of chlorophyll catabolism. Furthermore, its function of cell death protection may require mitochondrial localization, at least in part. Whether PPIX is a direct substrate of ACD2 will require further biochemical experiments and metabolite analysis.

Protox is the target enzyme of most of diphenylether-type herbicides, such as oxyfluorfen. Several lines of herbicide-resistant cells were created by overproduction of mitochondrial Protox to prevent PPIX accumulation, even though the primary target of the herbicide is thought to be the chloroplast-localized Protox (Watanabe et al., 1998). In ACD2-overexpressing plants, we found increased mitochondrial localization of ACD2 when compared with the wild type. We speculate that the protection of ACD2-overexpressing plants from PCD may be related to an increase in the amount of ACD2 in mitochondria.

Organellar Events in PCD

We previously found mitochondrial membrane potential loss to be a common early marker and often an essential event in PCD induced by several stimuli (Yao et al., 2004). Here, we found a number of additional organelle-associated events that occur prior to cell death induced by PPIX or light (in the case of *acd2*). Examination of the timing of and requirements for different events permits a provisional description of the cell autonomous plant PCD process. The earliest event we documented was a mitochondrial oxidative burst. This burst was essential for PCD. The oxidative burst was followed by NO accumulation in chloroplasts, changes in mitochondria and chloroplast positions and shapes, and the loss of mitochondrial membrane potential. H_2O_2 and/or NO have been implicated in PCD induction and spreading in plants (reviewed in Greenberg and Yao, 2004). However, in our conditions, H_2O_2 played a major role, whereas NO did not significantly contribute to PCD. Interestingly, Bethke et al. (2004) found that blocking NO accumulation promoted PCD in barley (*Hordeum vulgare*) aleurone cells.

Pathogen infection likely causes similar cellular changes to those caused by PPIX treatment of the wild type or light treatment of *acd2*. We saw similar apoptotic-like morphological changes in response to PPIX and *P. syringae* infection (both virulent and avirulent with different timing). Furthermore, *P. syringae* infection induces a mitochondrial oxidative burst (our unpublished data). Cell death events may be more complex during infection than in response to PPIX in the wild type or light in *acd2*. ACD2 and tAPX together affect the amount of cell death during infection. However, tAPX did not protect *acd2* cells from

light-induced cell death, although it blocked chloroplast production of H_2O_2. Cell death during infection appears to involve both chloroplast events (where tAPX and ACD2 are) as well as mitochondria (another site of ACD2 localization). A major challenge for the future is determining the specific molecules and events in the different organelles that contribute to the PCD process and determining how these events also influence the replication of pathogens.

METHODS

Materials

All *Arabidopsis thaliana* plant materials employed for this study were in the Columbia background. *acd2-2* (Greenberg et al., 1994), 35S:*ACD2* (Mach et al., 2001), and plants overexpressing thylakoidal ascorbate peroxidase (35S:tAPX, line 14/2) (Murgia et al., 2004) or expressing mitochondria-localized GFP (35S:β-ATPase-GFP; Logan and Leaver, 2000) were described previously. We generated *acd2* mutant plants homozygous for β-ATPase-GFP or tAPX by crossing the *acd2* mutant with 35S:β-ATPase-GFP or 35S:tAPX homozygous plants, respectively. Isolation of plants homozygous for *acd2* and the respective transgene was done by identifying *acd2* homozygous individuals in the F2 generation (plants with spontaneous lesions) and testing the progeny of these plants for kanamycin resistance. For plants overexpressing both ACD2 and tAPX, we used F1 plants from a cross between 35S:ACD2 and 35S:tAPX homozygotes. PPIX disodium salt was from Frontier Scientific. Oxyfluorfen and paraquat were from Sigma-Aldrich. CM-H_2DCFDA (5-and-6-chloromethyl-2′,7′-dichlorodi-hydrofluorescein diacetate, acetyl ester), DAF-FM diacetate (4-amino-5-methylamino-2′,7′-difluorofluorescein diacetate), MitoTracker Red CMXRos (CMXRos), and cPTIO [2-(4-carboxyphenyl)-4,4,5,5-tetra-methylimidazoline-1-oxyl-3-oxide] were obtained from Molecular Probes.

Pathogen Infections

Bacterial strains used were derived from *Pseudomonas syringae* pv *maculicola* strain DG3 (a *recA* derivative of ES4326) and *Pma* strain DG6 (an ES4326 *recA* derivative expressing the type-III effector *avrRpt2*) as described previously (Guttman and Greenberg, 2001). Bacterial culturing, syringe inoculations, and growth curve procedures were as described by Greenberg et al. (2000). Bacteria used for growth determination in planta were inoculated at OD_{600} of 0.0001.

For electron microscopy samples, 3-week-old wild-type leaves were inoculated with an avirulent pathogen *Pma* DG6 (carrying *avrRpt2*) at $OD_{600} = 0.005$ and a virulent pathogen *Pma* DG3 at $OD_{600} = 0.01$. Twelve to twenty-four hours after inoculation, leaves were fixed for electron microscopy analysis.

Immunolocalization

Leaf and root segments of wild-type and *acd2* mutant plants were fixed in 2.5% (v/v) glutaraldehyde and 2.0% (v/v) paraformaldehyde with 0.1 M cacodylate buffer, pH 7.2, overnight at 4°C. The samples were washed in the same buffer, dehydrated in a graded ethanol series, and then embedded in LR White resin (Electron Microscopy Sciences). Ultrathin sections were cut, collected on collodion-covered nickel grids, and then treated with blocking BSA-TBS buffer (0.87% [w/v] NaCl and 0.605% [w/v] Tris, pH 7.4, plus 1% [w/v] BSA) for 1 h. Sections were incubated with the anti-ACD2 antiserum at a concentration of 1:50 in BSA-TBS for 2 h at room temperature. After rinsing in BSA-TBS, bound primary antibody was detected using goat-anti-rabbit IgG labeled with 10-nm colloidal gold (Electron Microscopy Sciences). After washing in BSA-TBS and deionized water, specimens were stained with uranyl acetate and lead citrate before observation under a transmission electron microscope (Philips CM-120; FEI Company) at an accelerating voltage of 120 kV.

For statistical analysis of protein localization, ultrathin cross sections of the samples were prepared from three different blocks. Twenty-five cells were photographed in each of the treatments. The density of immunogold particles per area (μm) was counted as described previously (Yao et al., 2001).

Protoplast Preparation and Treatments

Leaf protoplasts were isolated from 15- to 20-d-old plants as described previously (Liang et al., 2003). For root protoplasts, 26-d-old root tissue from soil grown plants was used. Specifically, roots at the bottom of the pots were excised, washed, and subjected to protoplast isolation in dark condition. Protoplasts were treated with the indicated chemicals and incubated at 22°C under fluorescent lights as described (Yao et al., 2004). The percentage of survival of protoplasts after treatments was determined by fluorescein diacetate (Yao et al., 2004) staining using a hemacytometer (Hausser Scientific Company) under an Axioskop microscope (Carl Zeiss).

Live Imaging of Organelle Movements and ROS and NO Production

Microscopy observation in Figures 4, 5, 7, and 9 was performed using a confocal laser scanning microscope system (Leica TCS SP2 AOBS) with a ×63 (numerical aperture 1.4) glycerol objective. GFP, CM-H_2DCFDA, and DAF-FM signals were visualized with excitation at 488 nm (emission: 498 to 532 nm). CMXRos signals were visualized with excitation at 543 (495 to 635 nm), and chloroplast autofluorescence (488-nm excitation) was visualized at 738 to 793 nm. CM-H_2DCFDA and DAF-FM were dissolved in DMSO, and the final concentrations were 500 nM and 1 μM, respectively. Both control and treatment images were observed by z series stacking. The images shown in the figures were cross sections in the middle of cells, which were similar in size.

Cellular Fractionation

Roots of soil-grown plants (5 to 10 g) were rinsed in distilled water, blotted to remove excess water, and homogenized using a pestle and mortar in a buffer containing 25 mM MOPS, pH 7.5, 20 mM sodium ascorbate, 0.25% BSA (w/v), 0.4 M mannitol, 10 mM NaCl, 10 mM mercaptoethanol, 1 mM EDTA, and 0.6% polyvinylpyrrolidone. The homogenates were filtered through two layers of Miracloth (Calbiochem). The crude plastid fraction was centrifuged at 370*g* for 10 min at 4°C and was purified on 20 to 80% Percoll gradient according to Wimmer et al. (1997). The supernatant of the 370*g* was recentrifuged at 12,000*g* for 15 min. The pellet (crude mitochondria) was collected and further purified on 20 to 60% Percoll gradient according to Mach et al. (2001). Plastid fractions were analyzed for the respective enzyme marker glucose-6-P dehydrogenase following Journet and Douce (1985). Mitochondrial purity was assessed by staining with the mitochondria-specific dye MitoTracker Red CMXRos (Mach et al., 2001).

Protein Gel Blotting

Polyclonal anti-ACD2 antibody was used for protein gel blotting as described previously (Mach et al., 2001).

Trypan Blue Staining

Leaves were stained with trypan blue to visualize dead cells in fresh tissue as previously described (Rate et al., 1999).

Accession Numbers

Sequence data from this article can be found in the GenBank/EMBL data libraries under accession numbers AT4G37000 for *ACD2* and X98926 for tAPX.

Supplemental Data

The following material is available in the online version of this article.

Supplemental Figure 1. Mitochondrial Localization of ACD2 during Infection.

ACKNOWLEDGMENTS

We thank Laurens Mets, Stefan Hortensteiner, and members of the Greenberg lab for helpful discussions, Hua Lu and Hua Liang for comments on the manuscript, and Yang Liu for help with the confocal microscopy. We also thank Irene Murgia and David Logan for supplying tAPX and β-ATPase-GFP seeds. This work was supported by National Institutes of Health Grant 5R01 GM54292 to J.T.G.

Received July 20, 2005; revised November 11, 2005; accepted November 30, 2005; published December 30, 2005.

REFERENCES

Asai, T., Stone, J.M., Heard, J.E., Kovtun, Y., Yorgey, P., Sheen, J., and Ausubel, F.M. (2000). Fumonisin B1-induced cell death in Arabidopsis protoplasts requires jasmonate-, ethylene-, and salicylate-dependent signaling pathways. Plant Cell **12,** 1823–1835.

Bereiter-Hahn, J., and Vöth, M. (1994). Dynamics of mitochondria in living cells: Shape changes, dislocations, fusion, and fission of mitochondria. Microsc. Res. Tech. **27,** 198–219.

Bernardi, P., Petronilli, B., Lisa, F.D., and Forte, M. (2001). A mitochondrial perspective on cell death. Trends Biochem. Sci. **26,** 112–117.

Bethke, P.C., Badger, M.R., and Jones, R.L. (2004). Apoplastic synthesis of nitric oxide by plant tissues. Cell **16,** 332–341.

Bus, J.S., Aust, S.D., and Gibson, J.E. (1974). Superoxide- and singlet oxygen-catalyzed lipid peroxidation as a possible mechanism for paraquat (methyl viologen) toxicity. Biochem. Biophys. Res. Commun. **58,** 749–755.

Chew, O., Whelan, J., and Millar, A.H. (2003). Molecular definition of the ascorbate-glutathione cycle in Arabidopsis mitochondria reveals dual targeting of antioxidant defense in plants. J. Biol. Chem. **278,** 46869–46877.

Clarke, A., Desikan, R., Hurst, R.D., Hancock, J.T., and Neill, S.J. (2000). NO way back: Nitric oxide and programmed cell death in *Arabidopsis thaliana* suspension cultures. Plant J. **24,** 667–677.

Delledonne, M., Xia, Y., Dixon, R.A., and Lamb, C. (1998). Nitric oxide functions as a signal in plant disease resistance. Nature **394,** 585–588.

del Pozo, O., Pedley, K., and Martin, G. (2004). MAPKKKα is a positive regulator of cell death associated with both plant immunity and disease. EMBO J. **23,** 3072–3082.

Dietrich, R.A., Delaney, T.P., Uknes, S.J., Ward, E.R., Ryals, J.A., and Dangl, J.L. (1994). Arabidopsis mutants simulating disease resistance response. Cell **77,** 565–577.

Epple, P., Mack, A.A., Morris, V.R.F., and Dangl, J.L. (2003). Antagonistic control of oxidative stress-induced cell death in Arabidopsis by two related, plant-specific zinc finger proteins. Proc. Natl. Acad. Sci. USA **100,** 6831–6836.

Greenberg, J.T. (1997). Programmed cell death in plant-pathogen interactions. Annu. Rev. Plant Physiol. Plant Mol. Biol. **48,** 525–545.

Greenberg, J.T. (2005). Degrade or die: A dual role for autophagy in the plant immune response. Dev. Cell **8,** 799–801.

Greenberg, J.T., and Ausubel, F.M. (1993). Arabidopsis mutants compromised for the control of cellular damage during pathogenesis and aging. Plant J. **4,** 327–341.

Greenberg, J.T., Guo, A., Klessig, D.F., and Ausubel, F.M. (1994). Programmed cell death in plants, a pathogen-triggered response activated coordinately with multiple defense functions. Cell **77,** 551–563.

Greenberg, J.T., Silverman, F.P., and Liang, H. (2000). Uncoupling salicylic acid-dependent cell death and defense-related responses from disease resistance in the Arabidopsis mutant *acd5.* Genetics **156,** 341–350.

Greenberg, J.T., and Yao, N. (2004). The role and regulation of programmed cell death in plant-pathogen interactions. Cell. Microbiol. **6,** 201–211.

Guttman, D.S., and Greenberg, J.T. (2001). Functional analysis of type III effectors AvrRpt2 and AvrRpm1 of *Pseudomonas syringae* with the use of a single copy genomic integration system. Mol. Plant Microbe Interact. **14,** 145–155.

Hatsugai, N., Kuroyanagi, M., Yamada, K., Meshi, T., Tsuda, S., Kondo, M., Nishimura, M., and Hara-Nishimura, I. (2004). A plant vacuolar protease, VPE, mediates virus-induced hypersensitive cell death. Science **305,** 855–858.

Jacobs, J.M., and Jacobs, N.J. (1993). Porphyrinogen accumulation and export by isolated barley (*Hordeum vulgare* L.) plastids: Effect of diphenyl ether herbicides. Plant Physiol. **101,** 1181–1187.

Journet, E.P., and Douce, R. (1985). Enzymatic capacities of purified cauliflower bud plastids for lipid synthesis and carbohydrate metabolism. Plant Physiol. **79,** 458–467.

Kariola, T., Brader, G., Li, J., and Palva, E.T. (2005). Chlorophyllase 1, a damage control enzyme, affects the balance between defense pathways in plants. Plant Cell **17,** 282–294.

Kriska, T., Korytowski, W., and Girotti, A.W. (2002). Hyperresistance to photosensitized lipid peroxidation and apoptotic killing in 5-aminolevulinate-treated tumor cells overexpressing mitochondrial GPX4. Free Radic. Biol. Med. **15,** 1389–1402.

Lee, H.J., Duke, M.V., and Duke, S.O. (1993). Cellular localization of protoporphyrinogen-oxidizing activities of etiolated barley (*Hodeum vulgare L.*) leaves (relationship to mechanism of action of protoporphyrinogen oxidase-inhibiting herbicides). Plant Physiol. **102,** 881–889.

Lermontova, I., Kruse, E., Mock, H.P., and Grimm, B. (1997). Cloning and characterization of a plastidal and mitochondrial isoform of tobacco protoporphyrinogen IX oxidase. Proc. Natl. Acad. Sci. USA **94,** 8895–8900.

Liang, H., Yao, N., Song, J.T., Luo, S., Lu, H., and Greenberg, J.T. (2003). Ceramides modulate programmed cell death in plants. Genes Dev. **17,** 2636–2641.

Liu, Y., Schiff, M., Cyzmmek, K., Talloczy, Z., Levine, B., and Dinesh-Kumar, S.P. (2005). Autophagy regulates programmed cell death during the plant innate immune response. Cell **121,** 567–577.

Logan, D.C., and Leaver, C.J. (2000). Mitochondria-targeted GFP highlights the heterogeneity of micochondrial shape, size and movement within living plant cells. J. Exp. Bot. **51,** 865–871.

Mach, J.M., Castillo, A.R., Hoogstraten, R., and Greenberg, J.T. (2001). The Arabidopsis-accelerated cell death gene *ACD2* encodes red chlorophyll catabolite reductase and suppresses the spread of disease symptoms. Proc. Natl. Acad. Sci. USA **98,** 771–776.

Mateo, A., Muhlenbock, P., Rusterucci, C., Chang, C.C., Miszalski, Z., Karpinska, B., Parker, J.E., Mullineaux, P.M., and Karpinski, S. (2004). LESION SIMULATING DISEASE 1 is required for acclimation to conditions that promote excess excitation energy. Plant Physiol. **136,** 2818–2830.

Matile, P., Hortensteiner, S., and Thomas, H. (1999). Chlorophyll degradation. Annu. Rev. Plant Physiol. Plant Mol. Biol. **50,** 67–95.

Matsumoto, H., Kashimoto, Y., and Warabi, E. (1999). Basis for common chickweed (*Stellaria media*) tolerance to oxyfluorfen. Pestic. Biochem. Physiol. **64,** 47–53.

Mou, Z., Fan, W., and Dong, X. (2003). Inducers of plant systemic acquired resistance regulate NPR1 function through redox changes. Cell **27,** 935–944.

Murgia, I., Tarantino, D., Vannini, C., Bracale, M., Carravieri, S., and Soave, C. (2004). *Arabidopsis thaliana* plants overexpressing thylakoidal ascorbate peroxidase show increased resistance to paraquat-induced photooxidative stress and to nitric oxide-induced cell death. Plant J. **38,** 940–953.

Pruzinska, A., Tanner, G., Anders, I., Roca, M., and Hortensteiner, S. (2003). Chlorophyll breakdown: Pheophorbide *a* oxygenase is a Rieske-type iron-sulfur protein, encoded by the *accelerated cell death 1* gene. Proc. Natl. Acad. Sci. USA **100,** 15259–15264.

Rate, D.N., Cuenca, J.V., Bowman, G.R., Guttman, D.S., and Greenberg, J.T. (1999). The gain-of-function Arabidopsis *acd6* mutant reveals novel regulation and function of the salicylic acid signaling pathway in controlling cell death, defenses, and cell growth. Plant Cell **11,** 1695–1708.

Rodoni, S., Muhlecker, W., Anderl, M., Krautler, B., Moser, D., Thomas, H., Matile, P., and Hortensteiner, S. (1997). Chlorophyll breakdown in senescent chloroplasts, cleavage of pheophorbide a in two enzymatic steps. Plant Physiol. **115,** 669–676.

Taylor, N.L., Rudhe, C., Hulett, J.M., Lithgow, T., Glaser, E., Day, D.A., Millar, H., and Whealan, J. (2003). Environmental stresses inhibit and stimulate different protein import pathways in plant mitochondria. FEBS Lett. **547,** 125–130.

Wagner, D., Przybyla, D., Op den Camp, R., Kim, C., Landgraf, F., Lee, K.P., Würsch, M., Laloi, C., Nater, M., Hideg, E., and Apel, K. (2004). The genetic basis of singlet oxygen-induced stress responses of *Arabidopsis thaliana.* Science **306,** 1183–1185.

Walters, R.G., Ibrahim, D.G., Horton, P., and Kruger, N.J. (2004). A mutant of Arabidopsis lacking the triose-phosphate/phosphate translocator reveals metabolic regulation of starch breakdown in the light. Plant Physiol. **135,** 891–906.

Watanabe, N., Che, F.-S., Iwano, M., Takayama, S., Nakano, T., Yoshida, S., and Isogai, A. (1998). Molecular characterization of photomixotrophic tobacco cells resistant to protoporphyrinogen oxidase-inhibiting herbicides. Plant Physiol. **118,** 751–758.

Watanabe, N., Che, F.-S., Iwano, M., Takayama, S., Yoshida, S., and Isogai, A. (2001). Dual targeting of spinach protoporphyrinogen oxidase II to mitochondria and chloroplasts by alternative use of two in-frame initiation codons. J. Biol. Chem. **276,** 20474–20481.

Wimmer, B., Lottspeich, F., Van der Klei, I., Veenhuis, M., and Gietl, C. (1997). The glyoxisomal and plastid molecular chaperones (70-kDa heat shock protein) of watermelon cotyledons are encoded by a single gene. Proc. Natl. Acad. Sci. USA **94,** 13624–13629.

Wüthrich, K.L., Bovet, L., Hunziker, P.E., Donnison, I.S., and Hortensteiner, S. (2000). Molecular cloning, functional expression and characterisation of RCC reductase involved in chlorophyll catabolism. Plant J. **21,** 189–198.

Yang, M., Wardzala, E., Johal, G.S., and Gray, J. (2004). The wound-inducible *Lls1* gene from maize is an orthologue of the Arabidopsis *ACD1* gene, and the LLS1 protein is present in non-photosynthetic tissues. Plant Mol. Biol. **54,** 175–191.

Yao, N., Eisfelder, B., Marvin, J., and Greenberg, J.T. (2004). The mitochondrion—An organelle commonly involved in programmed cell death in *Arabidopsis thaliana.* Plant J. **40,** 596–610.

Yao, N., Tada, Y., Park, P., Nakayashiki, H., Tosa, Y., and Mayama, S. (2001). Novel evidence for apoptotic cell response and differential signals in chromatin condensation and DNA cleavage in victorin-treated oats. Plant J. **28,** 13–26.